Published in final edited form as:
Phys Rev B Condens Matter Mater Phys. 2012 September 21; 86(10): . doi:10.1103/PhysRevB.86.104428.

Measuring central-spin interaction with a spin-bath by pulsed ENDOR: Towards suppression of spin diffusion decoherence

S. J. Balian[1,*], **M. B. A. Kunze**[2], **M. H. Mohammady**[1], **G. W. Morley**[3], **W. M. Witzel**[4], **C. W. M. Kay**[2,5], and **T. S. Monteiro**[1]

[1]Department of Physics and Astronomy, University College London, Gower Street, London WC1E 6BT, United Kingdom

[2]Institute of Structural and Molecular Biology, University College London, Gower Street, London WC1E 6BT, United Kingdom

[3]Department of Physics, University of Warwick, Gibbet Hill Road, Coventry CV4 7AL, United Kingdom

[4]Sandia National Laboratories, Albuquerque, New Mexico 87185, USA

[5]London Centre for Nanotechnology, University College London, 17-19 Gordon Street, London WC1H 0AH, United Kingdom

Abstract

We present pulsed electron-nuclear double resonance (ENDOR) experiments which enable us to characterize the coupling between bismuth donor spin-qubits in Si and the surrounding spin-bath of ^{29}Si impurities which provides the dominant decoherence mechanism (nuclear spin diffusion) at low temperatures (< 16 K). Decoupling from the spin-bath is predicted and cluster correlation expansion simulations show near-complete suppression of spin diffusion, at optimal working points. The suppression takes the form of sharply peaked divergences of the spin diffusion coherence time, in contrast with previously identified broader regions of insensitivity to classical fluctuations. ENDOR data shows anisotropic contributions are comparatively weak, so the form of the divergences is independent of crystal orientation.

I. INTRODUCTION

Quantum decoherence presents a fundamental limitation to the realization of practical quantum computing and of other technological devices which actively exploit quantum phenomena. In 2002, a ground-breaking study established the usefulness of so-called optimal working points (OWPs):[1] these are parameter regimes where the system becomes – to first order – insensitive to fluctuations of external classical fields. We consider here the effect of OWPs in a system where decoherence of a central spin system arises from interactions with a fluctuating bath of surrounding spins; a scenario that is of considerable significance in the field of quantum information.[2–10]

A promising approach for silicon-based quantum information processing (QIP) involves combined electron and nuclear spins of donor atoms in Si, which are amenable to high-fidelity manipulation by means of electron paramagnetic resonance (EPR) and nuclear magnetic resonance (NMR) respectively. Most studies have considered phosphorus (^{31}P)

*balian@ucl.ac.uk.

PACS numbers: 76.70.Dx, 76.30.–v, 03.65.Yz, 03.67.Lx

Europe PMC Funders Author Manuscripts

donors in Si.[11–22] More recently, several different groups have investigated another Group V donor, ^{209}Bi. These studies not only showed that bismuth donors have similar properties to Si:P, such as long coherence times T_2 of the order of several ms at low temperatures (< 16 K),[23,24] but that they also offer new possibilities for QIP. For example, strong optical hyperpolarization was demonstrated,[23,25] allowing for efficient initialization of the nuclear spin. The Si:Bi spin system has an electron spin $S = 1/2$ and a large nuclear spin $I = 9/2$ as well as an atypically strong hyperfine coupling constant, $A/2\pi = 1.4754$ GHz. The strong state-mixing occurring for magnetic fields $B \simeq 0.1 – 0.6$ T where the hyperfine interaction competes with the electronic Zeeman energy, allows transitions which are forbidden at high magnetic fields,[26,27] observed recently in Ref. 28. In Refs. 26,27, a set of minima and maxima were found in the $f – B$ parameter space of dipole-allowed transitions at frequencies f. These $df/dB = 0$ points were identified as OWPs: line narrowing and reduced sensitivity to temporal and spatial noise in B over a broad region of fields (closely related to $df/dB = 0$ extrema), were found. However, to date, their effectiveness for reducing decoherence in the real environment of a spin-bath remains untested.

In natural Si, 4.67% of lattice sites are occupied by the nuclear spin-half ^{29}Si isotope, rather than the spinless ^{28}Si. Flip-flopping of the ^{29}Si spins provides the dominant mechanism of decoherence for both Si:P and Si:Bi systems at low temperatures. The decay of the donor Hahn spin echo for these systems is typically fitted to $\exp[-t/T_2 – (t/T_{SD})^n]$, where $T_{SD} < 1$ ms characterizes the nuclear spin diffusion, with $n \simeq 2 – 3$.[29] Other relaxation processes, such as those arising from donor-donor interactions, are represented by T_2. Since $T_2 >> T_{SD}$, nuclear spin diffusion remains the main channel of decoherence at low temperatures.[30,31]

In this work, we investigate the nature of the Bi-^{29}Si interaction by means of pulsed ENDOR.[32] To obtain an ENDOR spectrum, an EPR spin echo is detected as a function of a radio frequency (rf) excitation. When the rf radiation is resonant with an NMR transition, changes are seen in the EPR signal if the populations of the relevant energy levels change. Previous ENDOR studies of Si:Bi used rf frequencies of at least several hundreds of MHz,[23,24] and thus could not probe the weak couplings to a spin-bath. In contrast, here, rf frequencies of a few MHz were used. With this approach, we have measured the bismuth spin-bath superhyperfine (SHF) couplings and determined their anisotropy.

We also present the results of cluster correlation expansion (CCE) simulations.[29,33] This model has been used with considerable success to model central spin decoherence in Si:P.[4,6,7,29] In Ref. 24, weak state-mixing in Si:Bi was investigated by simply allowing for the variation of an effective gyromagnetic ratio. Here we adapt the CCE simulations to include, for the first time, the strong state-mixing seen near the OWPs. A key finding is the demonstration of near-complete suppression of nuclear spin diffusion, even in natural Si: this occurs in extremely narrow regions, where T_{SD} is in effect divergent,[34] in contrast to the broader effect expected from the form of df/dB.[1] A successful means of controlling decoherence is to employ isotopically enriched samples,[4,6,14,19,20,30,31,35–37] which can exhibit long T_2 times up to the order of seconds.[31] Thus, the OWPs represent a potentially complementary technique, effective for both natural Si and partially enriched samples. In addition, our work suggests that the OWPs may also be effective in suppressing residual effects such as donor-donor interactions which are responsible for shortening T_2 times from seconds to the ms timescale.[26]

II. SPIN HAMILTONIAN

We investigate a spin system with total Hamiltonian:

$$\widehat{H}=A\widehat{\mathrm{I}}\cdot\widehat{\mathrm{S}}+\widehat{H}_{\mathrm{Zee}}+\widehat{H}_{\mathrm{int}}+\widehat{H}_{\mathrm{bath}}. \quad 1$$

The first term denotes the isotropic hyperfine interaction between the bismuth electronic and nuclear spins. For Si:Bi, the usual high-field reduction to Ising form $A\widehat{\mathbf{I}}\cdot\widehat{\mathbf{S}}\simeq A\widehat{I}^{z}\widehat{S}^{z}$ cannot be made at the fields of interest here. The second term represents the Zeeman interaction with the external field, including the donor spins and summed over bath spins,

$$\widehat{H}_{\mathrm{Zee}}=\omega_0\left(\widehat{S}^{z}-\delta_{\mathrm{Bi}}\widehat{I}^{z}-\delta_{\mathrm{Si}}\sum_{n}\widehat{I}_{n}^{z}\right). \quad 2$$

Here, $\omega_0=\mu B/\hbar$ is the electronic Zeeman frequency (μ = 1.857 × 10^{-23} JT^{-1}) while δ_{Bi} = 2.486 × 10^{-4} and δ_{Si} = 3.021 × 10^{-4} are the ratios of the nuclear to electronic Zeeman frequencies for the donor and ^{29}Si spins respectively.

The spin-bath interaction term:

$$\widehat{H}_{\mathrm{int}}=\sum_{n}\widehat{\mathrm{I}}_{n}\mathrm{J}_{n}\widehat{\mathrm{S}}, \quad 3$$

represents the SHF couplings between the donor and bath spins, in general of tensor form (for anisotropic couplings). Finally, dipolar coupling between each pair of ^{29}Si spins is represented by the bath term,

$$\widehat{H}_{\mathrm{bath}}=\sum_{n<m}\widehat{\mathrm{I}}_{n}\mathrm{D}\,(\mathrm{r}_{nm})\,\widehat{\mathrm{I}}_{m}, \quad 4$$

where r_{nm} denotes the relative position vector of bath spins at lattice sites n and m. Writing $\mathrm{r}_{nm}\equiv\mathrm{r}$ for a pair of spins, the components of the dipolar tensor D are given by,

$$D_{ij}\,(\mathrm{r})=\left(\frac{\mu_0\delta_{\mathrm{Si}}^{2}\mu^{2}}{4\pi\hbar r^{3}}\right)\left(\delta_{ij}-3\frac{r_i r_j}{r^{2}}\right), \quad 5$$

with $\mu_0 = 4\pi \times 10^{-7}$ NA^{-2} and $i, j = x, y, z$.

III. ENDOR MEASUREMENTS

The experimental ENDOR studies reported here served to investigate and characterize the isotropic/anisotropic character of the spin-bath interaction term, namely a set of distinct $\mathbf{J}_n$ values – SHF couplings – in Eq. (3), corresponding to occupancy of inequivalent lattice sites by ^{29}Si impurities. Pulsed ENDOR experiments were performed using the Davies ENDOR pulse sequence.[32,38] We applied the pulse sequence $\pi_{\mathrm{mw}}-\tau_1-\pi_{\mathrm{rf}}-\tau_2-\frac{\pi}{2}\mathrm{mw}-\tau_3-\pi_{\mathrm{mw}}-\tau_3-\mathrm{echo}$, where the microwave (mw) frequency is chosen to excite one EPR transition and the rf is stochastically varied between 2 – 12 MHz or 2 – 7 MHz to excite all nuclear spin transitions in this region. We used 256 ns long π_{mw}-pulses and a 128 ns long $\frac{\pi}{2}$mw-pulse. For optimal signal-to-noise ratio and resolution, we used a π_{rf}-pulse of 10 μs. Pulse delays were set to τ_1 = 1 μs, τ_2 = 3 μs and τ_3 = 1.5 μs and a shot repetition time of 1.3 ms was employed to give a good signal-to-noise ratio. All experiments were carried out at 15 K on an E580 pulsed EPR spectrometer (Bruker Biospin) equipped with pulsed ENDOR accessory (E560DP), a dielectric ring ENDOR resonator (EN4118X-MD4), a liquid helium flow cryostat (Oxford CF935) and an rf amplifier (ENI

A-500W). We used a donor concentration of 3×10^{15} cm^{-3} and the magnetic field was directed perpendicular to the [111] plane.

While not offering the higher frequency resolution attainable with continuous-wave ENDOR,[39,40] the pulsed ENDOR measurements permit us to adequately constrain and to demonstrate the reliability of the numerical simulations. In particular, we established that isotropic couplings to the spin-bath dominate the decoherence dynamics. While not the focus of this study, a further motivation is to investigate the feasibility of an alternative possibility for QIP: to simultaneously manipulate the ^{29}Si atoms as spin-half qubits, along with the donors.[41]

Measured ENDOR spectra at $f \cong 9.755$ GHz are presented in Fig. 1, together with a list of SHF couplings. For the magnetic field range $B \cong 0.1 - 0.6$ T in Fig. 1, there is significant mixing of the high-field Si:Bi energy eigenstates $|m_S, m_I\rangle$. The mixed eigenstates, $|\pm, m\rangle$, correspond to doublets (at most) of constant $m = m_S + m_I$:

$$|\pm, m\rangle = a_m^{\pm} \left|\pm\frac{1}{2}, m \mp \frac{1}{2}\right\rangle + b_m^{\pm} \left|\mp\frac{1}{2}, m \pm \frac{1}{2}\right\rangle, \quad 6$$

$$|a_m^{\pm}|^2 - |b_m^{\pm}|^2 = \frac{\Omega_m(\omega_0)}{\sqrt{\left(\Omega_m^2(\omega_0) + 25 - m^2\right)}} \equiv \gamma_m(\omega_0), \quad 7$$

where $\Omega_m(\omega_0) = m + \frac{\omega_0}{A}(1 + \delta_{\mathrm{Bi}})$ and m is an integer, $-5 \le m \le 5$. Such mixing leads to a complex EPR spectrum for bismuth with $df/dB = 0$ extrema. The minima correspond to transitions between states corresponding to adjacent avoided level crossings, of which there are four. The disparity between the electronic Zeeman and hyperfine energy scales and SHF energy scales means that the tensor coupling in Eq. (3) reduces to simpler form,

$$\widehat{H}_{\mathrm{int},l} \approx \left(\alpha_l \widehat{I}_l^z + \beta_l \widehat{I}_l^x\right) \widehat{S}^z, \quad 8$$

written for coupling to a single ^{29}Si at site l, where $\alpha_l = \left[(a_{\mathrm{iso},l} - T_l) + 3T_l^2 \cos^2\vartheta_l\right]$ and $\beta_l = 3T_l \sin\vartheta_l \cos\vartheta_l$ with $a_{iso,l}$ and T_l the isotropic and anisotropic parts of the molecular-frame SHF tensor respectively and ϑ_l the angle between the external field and the line connecting the bismuth site and site l. Non-secular terms involving $\widehat{S}^x$ and $\widehat{S}^y$ can be neglected.[32] Diagonalization of the resulting 2-dimensional Hamiltonian, and setting $T_l = 0$ for a purely isotropic coupling leads to a simple expression for the ENDOR resonance frequency for donor level $|\pm, m\rangle$:

$$\Delta_{\mathrm{iso},l}^{\pm,m}(\omega_0) = \frac{1}{2\pi}\left|-\omega_0\delta_{\mathrm{Si}} \pm \left(\frac{a_{\mathrm{iso},l}}{2}\right)\gamma_m(\omega_0)\right|. \quad 9$$

The above expression is in perfect agreement with full numerical diagonalization. The couplings in Fig. 1 were extracted from the measured spectra by fitting to the data Gaussians of equal width and using Eq. (9). The same expression and a single set of couplings gave excellent agreement with data at 10 different fields. In particular, the observed pattern of half a dozen highest frequency ^{29}Si resonances moving to a minimum at $B \cong 0.2$ T, then increasing again, is directly attributable to mixing of the states of the bismuth donor: i.e., here $\gamma_m(\omega_0)$ has a minimum.

Ten out of the twelve couplings extracted from data were found to be purely isotropic. The highest-field spectrum was measured for a range of crystal orientations and only three weak intensity lines showed orientation-dependent frequencies and hence anisotropy. Two are indicated by X_1 and X_2 in Fig. 1: the corresponding two couplings with non-zero anisotropy were found to have ($a_{\mathrm{iso},X1} \simeq 2.8$, $T_{X1} \simeq 2.4$) MHz and ($a_{\mathrm{iso},X2} \simeq 0.4$, $T_{X2} \simeq 2.8$) MHz by fitting the more general form of Eq. (9) with non-zero T. A previous ESEEM (electron spin echo envelope modulation) study identified a single anisotropic coupling,[42] attributed to E-shell (nearest neighbor) ^{29}Si. The third line we identify is fitted by coupling constants consistent with the anisotropic coupling in Ref. 42. For most crystal orientations, this line is masked by much higher intensity lines arising from isotropic couplings.

At fields where $\gamma_m(\omega_0)$ becomes small (this occurs close to the $df/dB = 0$ minima as shown in Refs. 26,27), Eq. (9) tends to the ^{29}Si Zeeman frequency $\delta_{\mathrm{Si}}\omega_0$. It is straightforward to extend Eq. (9) to the anisotropic case and show that the latter statement also holds for anisotropic couplings. In effect, at these points, the donor might be said to approximately decouple from the bath. For example, for the EPR transition $|12\rangle \rightarrow |9\rangle$, (labeling the eigenstates $|n = 1, 2,\ldots 20\rangle$ in increasing order of energy), $\gamma_m(\omega_0) = 0$ at $B = 157.9$ mT for level $|12\rangle$ and $B = 210.5$ mT for $|9\rangle$. We note that there is however no B-field value where both the upper and lower levels have $\gamma_m(\omega_0) = 0$: as we see below, this is not actually essential for complete suppression of spin diffusion. The actual OWP (where $df/dB = 0$) is at $B = 188.0$ mT, occurring when

$$\gamma_{-3}(\omega_0) + \gamma_{-4}(\omega_0) - \frac{2\delta_{\mathrm{Bi}}}{(1+\delta_{\mathrm{Bi}})} = 0. \quad (10)$$

IV. CLUSTER CORRELATION EXPANSION SIMULATIONS

In order to model the full dynamics, we assume that the temperature and donor concentrations are low enough so that phonon-induced decoherence and decoherence due to interactions between donors are negligible. The Hahn spin echo decay of a central donor electron coupled to the bismuth nucleus in a bath of ^{29}Si was calculated using the CCE.[33] Denoting the spin echo intensity by $L(t)$, let $L_S(t)$ be $L(t)$ computed including only spins in some set or "cluster" of bath spins S. The quantity $\tilde{L}_S(t)$ is defined as,

$$L(t) = \prod_S \tilde{L}_S(t), \quad (11)$$

where the product is over all clusters. Applying this definition to $L_S(t)$ and factoring out $\tilde{L}_S(t)$, an explicit form for the $\tilde{L}_S(t)$ is obtained in terms of the $L_S(t)$ and the $\tilde{L}_C(t)$ in subsets C of S,

$$\tilde{L}_S(t) = L_S(t) / \prod_{C \subset S} \tilde{L}_C(t). \quad (12)$$

The problem of calculating $L(t)$ is reduced into independent components each for a distinct cluster of bath spins. The exact solution to $L(t)$ is obtained if the $\tilde{L}_S(t)$ from all clusters are combined using Eq. (11) and the approximation to $L(t)$ up to a maximum cluster size of k is defined as,

$$L^{(k)}(t)=\prod_{|S|\le k}\tilde{L}_S(t), \quad 13$$

which involves calculating reduced problems for all clusters each containing at most k spins. Including up to $L^{(k=2)}(t)$ (2-cluster) is a good approximation to $L(t)$ when considering only dipolar interactions in the bath affecting the spin echo, as these are of the order of a few kHz and hence perturbative compared to the SHF interactions in the MHz range involving the donor electron. The CCE is exact, but not always convergent. We calculated the 2-cluster (k = 2) approximation to the CCE and obtained convergence for up to k = 3.

The Hahn echo sequence evolves the combined systembath state to time $t = 2\tau$:

$$|\psi(t=2\tau)\rangle = e^{-i\widehat{H}\tau}(\widehat{\sigma}_x \otimes 1_B)\, e^{-i\widehat{H}\tau}|\psi(t=0)\rangle, \quad 14$$

where $\widehat{\sigma}_x$ is the Pauli-X gate acting on the donor and 1_B denotes the bath identity. We assume that the time taken for a π-pulse is small compared to τ. The initial state was written as a product of the initial donor and bath states, the former chosen as an equal superposition of states $|12\rangle$ and $|9\rangle$. The donor subsystem is recovered after tracing over the bath and the modulus of the normalized off-diagonal element of the donor reduced density matrix is proportional to the intensity of the echo at time $t = 2\tau$. The reduced problem of the 2-cluster bath was solved for each of the four initial 2-product bath states and the average intensity obtained. 2-clusters were formed by pairing ^{29}Si spins separated by up to the 3rd nearest neighbor distance in a diamond cubic lattice of side length 160 Å. Convergence was obtained as the lattice size and the separation between the two bath nuclei were extended. It was assumed that B was large enough to conserve the total ^{29}Si Zeeman energy. Thus, the dipolar interaction between the two bath spins took the form of a combination of Ising ($\widehat{I}_1^z\widehat{I}_2^z$) and flip-flop ($\widehat{I}_1^+\widehat{I}_2^- + \widehat{I}_1^-\widehat{I}_2^+$) terms. The Kohn-Luttinger electronic wavefunction was used to calculate the isotropic Fermi contact SHF strength with an ionization energy of 0.069 eV for the bismuth donor. Calculated couplings were of the same order as those obtained from data. The data showed that isotropic couplings predominate; hence anisotropic couplings could be neglected and the simulations are insensitive to orientation. Finally, we obtained the average $L^{(k=2)}(t)$ over 100 spatial configurations of ^{29}Si occupying 4.67% of lattice sites. The resulting decay curves were fitted to $\exp[-t/T_2 - (t/T_{SD})_n]$, obtaining $T_2 >> T_{SD}$ and values of $n \simeq 2 - 3$.

V. SUPPRESSION OF NUCLEAR SPIN DIFFUSION

The results of our CCE simulations are presented in Fig. 2. Figure 2(a) shows the behavior around the B = 188.0 mT OWP, associated with the $|12\rangle \rightarrow |9\rangle$ EPR line. The calculated coherence time T_{SD} (orange dashed line) is superposed on a color map showing the SHF spectrum: the latter shows ENDOR spectra simulated as a function of B, using Eq. (9) and centered about the ^{29}Si nuclear Zeeman frequency. Strikingly, as B approaches the OWP, the "comb" of SHF lines narrows to little more than the width of a single line. This suggests a drastic reduction in the value of the SHF couplings, indicating that the bismuth has become largely uncoupled from the ^{29}Si spin-bath.

The collapse in the SHF couplings is illustrated further in Fig. 2(b). The lower panel shows the measured spectrum at 9.755 GHz. Using our experimentally-determined SHF couplings, the corresponding spectrum at the OWP is shown in the upper panel of Fig. 2(b),

Europe PMC Funders Author Manuscripts

demonstrating clearly the line narrowing (corresponding to the same parameters as Fig. 2(a) but at the precise field value of the OWP).

The behavior of T_{SD} is also quite striking and unexpected: the coherence time predicted by CCE simulations increases asymptotically at the OWP by several orders of magnitude. Away from the OWP, the results agree well with experimentally measured values of approximately 0.7 ms.[24] In Ref. 24, in a regime of weak state-mixing, simulations using an effective gyromagnetic ratio indicated that T_{SD} was slightly reduced (by about 5%) in a regime corresponding to lower *df/dB*. The present study on the other hand, (which in contrast to Ref. 24 employed a full treatment of the quantum eigenstate mixing) shows rather an effect very sharply peaked about the OWP: nuclear spin diffusion is predicted to be largely suppressed, but over an extremely narrow magnetic field range.

Figure 2(c) shows a sample of CCE spin echo decays from which T_{SD} times were extracted, and also serves to further illustrate the sharp increase in T_{SD}. Similar suppression is present for other OWPs in Si:Bi. There are *df/dB* = 0 minima for the $|15\rangle \rightarrow |6\rangle$, $|14\rangle \rightarrow |7\rangle$, $|13\rangle \rightarrow |8\rangle$, $|12\rangle \rightarrow |9\rangle$ and $|11\rangle \rightarrow |8\rangle$ transitions in the frequency range 5 – 7.5 GHz and two maxima for $|12\rangle \rightarrow |11\rangle$ and $|9\rangle \rightarrow |8\rangle$ close to 1 GHz. The decoupling from the spin-bath is also expected to lead to suppression of decoherence arising from the interaction with a bath of donors.[26]

VI. CONCLUSIONS

In conclusion, we present the first measurements of the isotropic SHF couplings which dominate the interaction between a bismuth donor and a bath of ^{29}Si impurities. We further demonstrate the suppression of couplings at OWPs. Finally, the spin echo decay of the donor is calculated as a many-body problem and sharp divergence of the spin diffusion time is observed at an OWP. Our study motivates experimental EPR studies in the range 5 – 7.5 GHz corresponding to the regions of suppressed decoherence.

Acknowledgments

We acknowledge Bernard Pajot for the Si:Bi crystal used here and thank the EPSRC for financial support through the COMPASSS grant. GWM is supported by the Royal Commission for the Exhibition of 1851. Sandia National Laboratories is a multiprogram laboratory operated by Sandia Corporation, a wholly owned subsidiary of Lockheed Martin Corporation, for the U.S. Department of Energy's National Nuclear Security Administration under contract DE-AC04-94AL85000.

References

1. Vion D, Aassime A, Cottet A, Joyez P, Pothier H, Urbina C, Esteve D, Devoret MH. Science. 2002; 296:886. [PubMed: 11988568]
2. de Sousa R, Das Sarma S. Phys. Rev. B. 2003; 67:033301.
3. de Sousa R, Das Sarma S. Phys. Rev. B. 2003; 68:115322.
4. Abe E, Itoh KM, Isoya J, Yamasaki S. Phys. Rev. B. 2004; 70:033204.
5. Takahashi S, Hanson R, van Tol J, Sherwin MS, Awschalom DD. Phys. Rev. Lett. 2008; 101:047601. [PubMed: 18764365]
6. Abe E, Tyryshkin AM, Tojo S, Morton JJL, Witzel WM, Fujimoto A, Ager JW, Haller EE, Isoya J, Lyon SA, Thewalt MLW, Itoh KM. Phys. Rev. B. 2010; 82:121201(R).
7. Witzel WM, Carroll MS, Morello A, Cywinski L, Das Sarma S. Phys. Rev. Lett. 2010; 105:187602. [PubMed: 21231138]
8. Bar-Gill N, Pham LM, Belthangady C, Le Sage D, Cappellaro P, Maze JR, Lukin MD, Yacoby A, Walsworth R. Nat. Commun. 2012; 3:858. [PubMed: 22617298]

9. Zhao N, Ho SW, Liu RB. Phys. Rev. B. 2012; 85:115303.
10. de Lange G, van der Sar T, Blok M, Wang Z-H, Dobrovitski V, Hanson Ronald. Sci. Rep. 2012; 2:382. [PubMed: 22536480]
11. Kane BE. Nature. 1998; 393:133.
12. Schofield SR, Curson NJ, Simmons MY, Rueß FJ, Hallam T, Oberbeck L, Clark RG. Phys. Rev. Lett. 2003; 91:136104. [PubMed: 14525322]
13. Stoneham AM, Fisher AJ, Greenland PT. J. Phys.: Condens. Matter. 2003; 15:L447.
14. Tyryshkin AM, Lyon SA, Astashkin AV, Raitsimring AM. Phys. Rev. B. 2003; 68:193207.
15. Fu K-MC, Ladd TD, Santori C, Yamamoto Y. Phys. Rev. B. 2004; 69:125306.
16. Morley GW, McCamey DR, Seipel HA, Brunel L-C, van Tol J, Boehme C. Phys. Rev. Lett. 2008; 101:207602. [PubMed: 19113380]
17. Morello A, Pla JJ, Zwanenburg FA, Chan KW, Tan KY, Huebl H, Möttönen M, Nugroho CD, Yang C, van Donkelaar JA, Alves ADC, Jamieson DN, Escott CC, Hollenberg LCL, Clark RG, Dzurak AS. Nature. 2010; 467:687. [PubMed: 20877281]
18. Greenland PT, Lynch SA, van der Meer AFG, Murdin BN, Pidgeon CR, Redlich B, Vinh NQ, Aeppli G. Nature. 2010; 465:1057. [PubMed: 20577211]
19. Simmons S, Brown RM, Riemann H, Abrosimov NV, Becker P, Pohl H-J, Thewalt MLW, Itoh KM, Morton JJL. Nature. 2011; 470:69. [PubMed: 21248751]
20. Steger M, Sekiguchi T, Yang A, Saeedi K, Hayden ME, Thewalt MLW, Itoh KM, Riemann H, Abrosimov NV, Becker P, Pohl H-J. J. Appl. Phys. 2011; 109:102411.
21. Dreher L, Hoehne F, Stutzmann M, Brandt MS. Phys. Rev. Lett. 2012; 108:027602. [PubMed: 22324708]
22. Fuechsle M, Miwa JA, Mahapatra S, Ryu H, Lee S, Warschkow O, Hollenberg LCL, Klimeck G, Simmons MY. Nature Nanotech. 2012; 7:242.
23. Morley GW, Warner M, Stoneham AM, Greenland PT, van Tol J, Kay CWM, Aeppli G. Nature Mater. 2010; 9:725–729. [PubMed: 20711180]
24. George RE, Witzel W, Riemann H, Abrosimov NV, Nötzel N, Thewalt MLW, Morton JJL. Phys. Rev. Lett. 2010; 105:067601. [PubMed: 20868014]
25. Sekiguchi T, Steger M, Saeedi K, Thewalt MLW, Riemann H, Abrosimov NV, Nötzel N. Phys. Rev. Lett. 2010; 104:137402. [PubMed: 20481913]
26. Mohammady MH, Morley GW, Monteiro TS. Phys. Rev. Lett. 2010; 105:067602. [PubMed: 20868015]
27. Mohammady MH, Morley GW, Nazir A, Monteiro TS. Phys. Rev. B. 2012; 85:094404.
28. Morley, GW.; Lueders, P.; Mohammady, MH.; Balian, SJ.; Aeppli, G.; Kay, CWM.; Witzel, WM.; Jeschke, G.; Monteiro, TS. e-print arXiv:1109.4269 (unpublished)
29. Witzel WM, Das Sarma S. Phys. Rev. B. 2006; 74:035322.
30. Tyryshkin AM, Morton JJL, Benjamin SC, Ardavan A, Briggs GAD, Ager JW, Lyon SA. J. Phys.: Condens. Matter. 2006; 18:S783.
31. Tyryshkin AM, Tojo S, Morton JJL, Riemann H, Abrosimov NV, Becker P, Pohl H-J, Schenkel T, Thewalt MLW, Itoh KM, Lyon SA. Nature Mater. 2012; 11:143. [PubMed: 22138791]
32. Schweiger, A.; Jeschke, G. Principles of Pulse paramagnetic resonance. Oxford University Press; Great Clarendon Street, Oxford, UK: 2001.
33. Yang W, Liu RB. Phys. Rev. B. 2008; 78:085315.Yang W, Liu RB. ibid. 2008; 78:129901(E).Yang W, Liu RB. ibid. 2009; 79:115320.
34. In the sense that decay of the spin echo is no longer discernible in our converged cluster calculations.
35. Steger M, Saeedi K, Thewalt MLW, Morton JJL, Riemann H, Abrosimov NV, Becker P, Pohl H-J. Science. 2012; 336:1280. [PubMed: 22679091]
36. Weis, CD.; Lo, CC.; Lang, V.; Tyryshkin, AM.; George, RE.; Yu, KM.; Bokor, J.; Lyon, SA.; Morton, JJL.; Schenkel, T. e-print arXiv:1202.1560 (unpublished)

37. Wolfowicz, G.; Simmons, S.; Tyryshkin, AM.; George, RE.; Riemann, H.; Abrosimov, NV.; Becker, P.; Pohl, H-J.; Lyon, SA.; Thewalt, MLW.; Morton, JJL. e-print arXiv:1207.3776 (unpublished)
38. Although Mims ENDOR offers higher selectivity to small SHF couplings, it would suffer from blind spots.
39. Feher G. Phys. Rev. 1959; 114:1219.
40. Hale EB, Mieher RL. Phys. Rev. 1969; 184:739.
41. Akhtar W, Filidou V, Sekiguchi T, Kawakami E, Itahashi T, Vlasenko L, Morton JJL, Itoh KM. Phys. Rev. Lett. 2012; 108:097601. [PubMed: 22463668]
42. Belli M, Fanciulli M, Abrosimov NV. Phys. Rev. B. 2011; 83:235204.

Europe PMC Funders Author Manuscripts

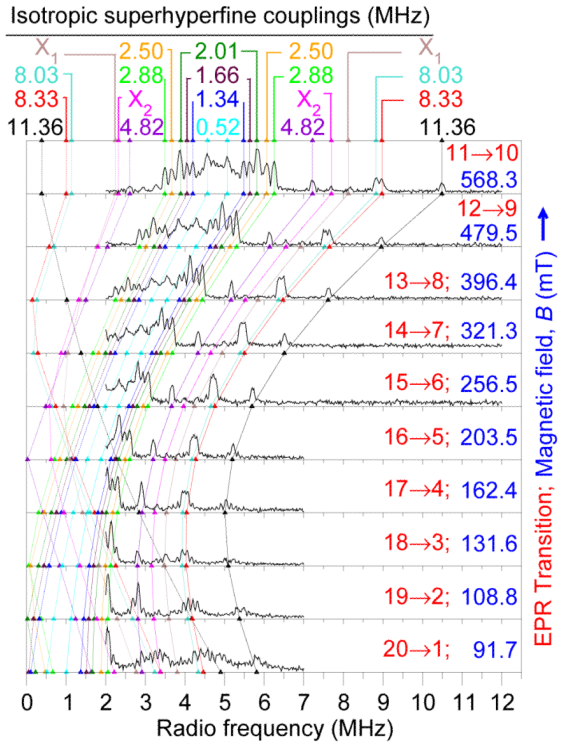

FIG. 1.

(color online) Pulsed ENDOR measured for bismuthdoped silicon with frequency 9.8 GHz at which ten EPR lines are observed, the resonance peaks due to interactions of the donor with ^{29}Si nuclei at inequivalent lattice sites. The isotropic superhyperfine couplings were extracted from the spectrum at the highest magnetic field. As the field is varied, the smooth lines follow the resonance positions according to Eq. (9). Solid and dotted lines distinguish between the two peaks observed for each coupling, each corresponding to one of the two donor levels involved in the EPR transition. Only the peaks labeled X_1 and X_2, in addition to a third pair not resolved here, were found to show anisotropy from performing ENDOR as a function of crystal orientation.

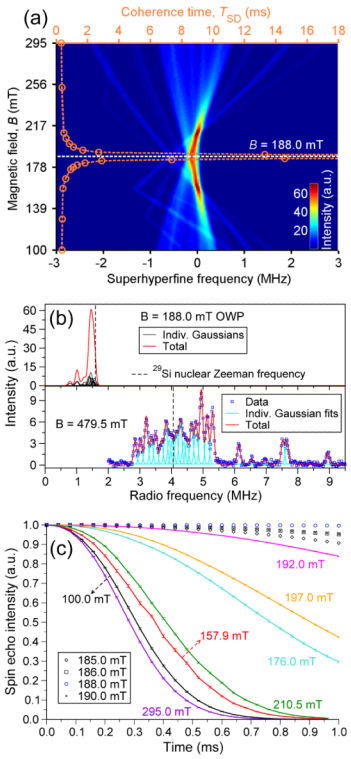

FIG. 2.

(color online) Suppression of Bi-^{29}Si spin-bath decoherence for the $|12\rangle \rightarrow |9\rangle$ EPR transition. (a) Simulated ENDOR and nuclear spin diffusion coherence times T_{SD} as a function of magnetic field B, showing collapse of the superhyperfine couplings and a sharp increase in T_{SD} as the field approaches the $B = 188.0$ mT optimal working point (OWP). The dashed line is a fit. (b) Simulated ENDOR at the $B = 188.0$ mT OWP (upper panel) and experimental spectrum at 9.755 GHz (lower panel). (c) Calculated donor Hahn spin echo decays from which coherence times in Fig. 2(a) were extracted.

Europe PMC Funders Author Manuscripts